Epilepsia Open the International League Against Epilepsy
Open Access
FULL-LENGTH ORIGINAL RESEARCH

Automated long-term EEG analysis to localize the epileptogenic zone

*†[1]Pieter van Mierlo, *[1]Gregor Strobbe, *‡Vincent Keereman, †Gwénael Birot, ‡Stefanie Gadeyne, †§Markus Gschwind, ‡Evelien Carrette, ‡Alfred Meurs, ¶Dirk Van Roost, ‡Kristl Vonck, §Margitta Seeck, †§[2]Serge Vulliémoz, and ‡[2]Paul Boon

Epilepsia Open, 2(3):322–333, 2017
doi: 10.1002/epi4.12066

Dr. Pieter van Mierlo is a postdoctoral fellow at the Functional Brain Mapping Lab of the University of Geneva, Switzerland and at the Medical Image and Signal Processing Group of Ghent University, Belgium.

Summary

Objective: **We investigated the performance of automatic spike detection and subsequent electroencephalogram (EEG) source imaging to localize the epileptogenic zone (EZ) from long-term EEG recorded during video-EEG monitoring.**

Methods: **In 32 patients, spikes were automatically detected in the EEG and clustered according to their morphology. The two spike clusters with most single events in each patient were averaged and localized in the brain at the half-rising time and peak of the spike using EEG source imaging. On the basis of the distance from the sources to the resection and the known patient outcome after surgery, the performance of the automated EEG analysis to localize the EZ was quantified.**

Results: **In 28 out of the 32 patients, the automatically detected spike clusters corresponded with the reported interictal findings. The median distance to the resection in patients with Engel class I outcome was 6.5 and 15 mm for spike cluster 1 and 27 and 26 mm for cluster 2, at the peak and the half-rising time of the spike, respectively. Spike occurrence (cluster 1 vs. cluster 2) and spike timing (peak vs. half-rising) significantly influenced the distance to the resection ($p < 0.05$). For patients with Engel class II, III, and IV outcomes, the median distance increased to 36 and 36 mm for cluster 1. Localizing spike cluster 1 at the peak resulted in a sensitivity of 70% and specificity of 100%, positive prediction value (PPV) of 100%, and negative predictive value (NPV) of 53%. Including the results of spike cluster 2 led to an increased sensitivity of 79% NPV of 55% and diagnostic OR of 11.4, while the specificity dropped to 75% and the PPV to 90%.**

Significance: **We showed that automated analysis of long-term EEG recordings results in a high sensitivity and specificity to localize the epileptogenic focus.**

KEY WORDS: **Automated spike detection, Automated spike localization, EEG source imaging, Patient-specific head model.**

Accepted May 22, 2017.

*Medical Image and Signal Processing Group, Department of Electronics and Information Systems, Ghent University–iMinds Medical IT Department, Ghent, Belgium; †Functional Brain Mapping Laboratory, Department of Fundamental Neurosciences, University of Geneva, Geneva, Switzerland; ‡Laboratory for Clinical and Experimental Neurophysiology, Neurobiology and Neuropsychology, Department of Neurology, Ghent University Hospital, Ghent, Belgium; §Epilepsy and EEG Unit, University Hospital of Geneva, Geneva, Switzerland; and ¶Department of Neurosurgery, Ghent University Hospital, Ghent, Belgium

Address correspondence to Pieter van Mierlo, Functional Brain Mapping Laboratory, Campus Biotech, Chemin des Mines 9, Genève 1202, Switzerland. E-mail: pieter.vanmierlo@ugent.be

[1]Authors contributed equally.
[2]Shared last authors.

Key Points

- Automated long-term EEG analysis localizes the epileptogenic zone with high sensitivity and specificity
- Automated EEG spike detection corresponded with the reported interictal findings
- The most occurring type of spikes localized significantly closer to the resection compared to the second most occurring ones
- Localization of the spike cluster with most detected events at the peak time was a predictor of favorable outcome

In patients with drug-resistant epilepsy, the aim of the presurgical evaluation is to identify the epileptogenic zone (EZ) on the basis of a combination of functional and anatomical imaging: video-electroencephalography (EEG) monitoring, structural magnetic resonance imaging (MRI), interictal positron emission tomography (PET), ictal single photon emission computed tomography (SPECT), magnetoencephalography (MEG), and neurophysiological testing.[1] The results of all performed investigations are combined to delineate the EZ prior to surgery. Correct delineation of the EZ is crucial for postsurgical outcome but remains a challenge using noninvasive techniques.[2]

EEG/MEG source imaging (ESI/MSI) analysis techniques allow providers to reconstruct the underlying brain activity based on recorded EEG and MEG signals[3] and have been successfully used in epilepsy.[4] ESI of scored interictal spikes, recorded with a standard clinical EEG setup (approximately 21–32 electrodes) and using a patient-specific head model, has a sensitivity of 64% and specificity of 54% to localize the EZ.[5] The same study shows that ESI of marked spikes recorded with high-density EEG increases the sensitivity to 84% and the specificity to 88%. Furthermore, in a follow-up study it has been shown that patients with concordant structural MRI and high-density ESI have a 92.3% (n = 24/26) probability of favorable outcome.[6] MSI of the epileptic spikes was concordant with the resection, in the same lobe, in 54–80% of the patients.[7] These findings were confirmed in a later study in 62 patients, where MSI had a sensitivity of 55% and a positive predictive value of 78%.[8]

Despite these encouraging results, ESI/MSI is part of the presurgical evaluation in only a limited number of epilepsy centers worldwide. A survey in the E-PILEPSY consortium (http://www.e-pilepsy.eu/) showed that only 12 out of 25 centers perform electromagnetic source imaging.[9] ESI is performed in 9 centers, and MSI is performed in 7 epilepsy centers. Of these epilepsy centers, 4 perform both ESI and MSI. All centers have their specific analysis strategy to localize the interictal spikes. Many different forward head models are used to perform ESI: spherical, multispherical, ellipsoid, and realistic, based either on a template MRI or on the patient's specific MRI. The inverse methods most commonly used are single dipole estimation, LORETA,[10] eLORETA,[11] sLORETA,[12] LAURA,[13] or MUSIC.[14] Each center has its own method of choice, mostly depending on working habit with the specific method.

The diversity of applied methods indicates that there is a lack of a standardized method to analyze the EEG and to perform ESI of interictal spikes. Automated EEG analysis would ensure reproducibility of the results and would allow epilepsy centers that do not have ESI/MSI expertise to incorporate this noninvasive technique in the presurgical evaluation without the need to acquire specific complex technical expertise and dedicated software.

We have designed a method to perform automated EEG analysis to localize the EZ. In the long-term EEG recordings, spikes are automatically detected and clustered. Subsequent automated ESI based on a realistic head model constructed from the patient's individual T1-MRI localizes the source of the spike clusters. In this study, the performance of this method to localize the EZ was investigated in 32 operated patients.

Methods

Patients

Twenty-three patients from Ghent University Hospital (PAT 1–23) and 9 from Geneva University Hospital (PAT 24–32) were included in the study. Inclusion criteria were: (1) patients who underwent presurgical evaluation and for whom long-term video-EEG monitoring data were available, (2) patients who received a one-time resective epilepsy surgery, (3) availability of structural MRI before and after resection, (4) follow-up of minimum 1 year postoperatively, and (5) patients who gave informed consent. From Ghent University Hospital all patients who had resective surgery after 2010 and met the inclusion criteria were included in this study. From Geneva University Hospital all patients from the previous study Birot et al.[15] were included if they had video-EEG monitoring at Geneva University Hospital and met the inclusion criteria. Collected patients' characteristics are described in Table 1.

EEG acquisition

The patients recruited from Ghent University Hospital underwent long-term video-EEG monitoring recorded with 27 electrodes. The 27-electrode setup consisted of 19 electrodes placed according to the international 10–20 system plus 8 additional electrodes: Fpz, Oz, T9, T10, TP9, TP10, and zygomatic electrodes T1 and T2 (as depicted in the left panel of Fig. S1). EEG was recorded using the Micromed system (Micromed Europe, Treviso, Italy) with a sampling rate of 256 Hz during 3 to 7 days.

Table 1. Patient details

PAT ID	Epilepsy type	Age at onset	Age at surgery	Video/EEG monitoring date	EEG duration	Interictal EEG findings	Ictal onset discharges	Surgery type	Resec vol (cm3)	Follow-up	Engel class
1	RFLE	8	30	5/05/2011–5/10/2011	60:00	Bilateral slow sharp waves	RF	R F & opercular topectomy	6.8	4 years	I
2	RTLE	5	48	9/1/2010–9/7/2010	53:55	RFT sharp waves	RFT	R SAH	21.4	3 years	I
3	RTLE	6	33	6/2/2011–6/9/2011	63:00	RFT IED	R	R SAH	5.9	3 years	I
4	RTLE	15	22	11/22/2010–11/30/2010	83:13	RFT IED	RFT	R SAH	6.3	3 years	I
5	RTLE	18	55	5/12/2011–5/19/2011	57:00	RFT IED and sharp waves	RFT-infT and centroPT (1 seizure)	R SAH + RT topectomy	21.2	2 years 9 months	I
6	LTLE	20	23	1/2/2012–1/6/2012	39:00	No IED	L	L mT (incl prepontine) lesionectomy	1.2	2 years 4 months	IV
7	RTLE	20	35	9/10/2011–9/17/2011	83:13	RFT IED	Bilateral	R basoT lesionectomy	1.3	1 year 6 months	I
8	RTLE	12	27	6/25/2012–7/2/2012	77:13	RFT IED and irregular slow waves	Bilateral and RFT	R SAH	1.9	2 year 5 months	I
9	RTLE	15	36	1/24/2012–1/31/2012	83:13	R slow waves and sharp waves	Bilateral and RF	R 2/3 T lobectomy	14.6	2 year 1 month	IV
10	LOLE	48	49	3/21/2013–3/28/2013	83:13	LF IED and LFT sharp waves	LPO and LT	L O lesionectomy	3.3	2 year 1 month	I
11	LTLE	19	54	1/30/2013–2/6/2013	21:44	LFT IED and RT IED	LT	L SAH	4.7	1 year 9 months	I
12	LTLE	18	28	2/12/2013–2/19/2013	72:49	LFT IED	L and bilateral (1 seizure)	L 2/3 T lobectomy + lesionectomy	41.3	1 year 8 months	I
13	RTLE	24	50	1/30/2013–2/6/2013 and 3/17/2013–3/24/2013	83:13	RFT IED	RFT	R SAH	4.8	1 year	I
14	RTLE	24	26	4/28/2009–5/2/2009	26:31	RFT IED	Bilateral FT	R 2/3 T lobectomy	48.3	5 year 5 months	I
15	LTLE	31	36	10/12/2009–10/17/2009	24:20	LFT IED	LFT	LT lesionectomy	2.6	4 year 8 months	I
16	LTLE	40	49	1/21/2008–1/27/2008	0:33	LFT IED and slow sharp waves	LFT	L 2/3 T lobectomy + basoT topectomy	34.6	3 years 11 months	I
17	RTLE	35	42	1/11/2010–1/15/2010	16:35	RFT IED and slow waves	RFT	R SAH	3.6	2 year 2 months	I
18	LTLE	36	40	12/15/2008–12/20/2008	41:31	No IED	LFT	L SAH	6.7	4 years	I
19	RTLE	16	55	11/30/2009–12/4/2009	8:26	RFT IED	Muscle artefact	R subinsular lesionectomy	5.9	4 years	II
20	RTLE	4	18	11/2/2009–11/5/2009	24:06	RFT IED	R	R SAH	3.8	4 years	I
21	LFTLE	4	11	2/22/2010–2/26/2010	90:50	L slow sharp waves	None	L FT and insular corticectomy	14.0	1 year 10 months	I
22	LTOLE	7	16	10/8/2012–10/10/2012	62:10	LFT IED	LTP	L O and Hipp lesionectomy	13.1	2 year 9 months	II
23	LTLE	31	43	10/1/2007–10/7/2007	1:29	LFT slow and sharp waves	L	L SAH	4.2	1 year	I
24	LPLE	3	9	1/5/2004–1/9/2004	8:54	CP slow and sharp waves	LCP	L P corticectomy	8.2	10 years	IV
25	RTLE	11	16	1/26/2009–1/30/2009	1:55	RT IED	RT	R 2/3 T lobectomy	27.2	5 years	I
26	LFLE	1	12	2/16/2009–2/20/2009	4:53	LCP IED	L FC	L F and C lesionectomy	25.8	5 years	I
27	LTLE	1	11	3/25/2008–4/3/2008	5:39	Bilateral FT IED and LT slow waves	LFT	L 2/3 T lobectomy excl. AH	32.9	8 years	I
28	RPTLE	8	11	2/5/2007–2/13/2007	8:25	RPO IED and bilateral FT IED	RPO	R T & P lobectomy	51.9	4 years	III
29	LTLE	1	12	5/31/2010–6/4/2010	3:49	Multifocal L IED	LFC	L T lobectomy	57.3	4 years	I

Continued

Table 1. Continued.

PAT ID	Epilepsy type	Age at onset	Age at surgery	Video/EEG monitoring date	EEG duration	Interictal EEG findings	Ictal onset discharges	Surgery type	Resec vol (cm3)	Follow-up	Engel class
30	RTLE	9	32	11/9/2009–11/13/2009	12:37	RT IED	LPO	R SAH	9.5	7 years	I
31	LTLE	13	34	10/15/2006–10/25/2006	3:41	LT IED	LT	L SAH	5.2	10 years	II
32	LTLE	8	18	7/11/2011–7/16/2011	7:30	Bilateral T IED, LTP bursts, and spike waves	LTP	L 2/3 T lobectomy	33.7	5 years	II

C, central; excl. AH, excluding amygdala and hippocampus; F, frontal; hipp, hippocampal; IED, interictal epileptiform discharge; incl, including; inf, inferior; L, left; LE, lobe epilepsy; O, occipital; P, parietal; R, right; SAH, selective amygdalohippocampectomy; T, temporal.

The 9 patients from the University Hospital of Geneva had long-term video-EEG monitoring acquired with 31 electrodes. These were the 19 electrode of the 10–20 system plus 12 additional electrodes FC1, FC2, FC5, FC6, CP1, CP2, CP5, CP6, TP9, TP10, and electrodes T1 and T2 on the cheek (as depicted in the right panel of Fig. S1). The EEG was recorded with the Deltamed system (Natus Medical, Pleasanton, CA, U.S.A.) with a sampling rate of 256 Hz.

Automated detection of spikes and subsequent EEG source imaging

The proposed method, Epilog PreOp (Epilog, Ghent, Belgium), consists of automatic spike detection followed by ESI of the different identified spike clusters, which contain detected spikes with similar morphology. The source localization is compared to the delineated resection area, and outcome measures to assess the performance of the method were calculated. The complete framework is shown in Fig. 1. In the next paragraphs we provide detailed information about the spike detection, ESI, and the outcome measures to evaluate the performance of the method.

Spike detection

All available EEG from the long-term video-EEG monitoring, that is, the EEG that was archived on the hospitals' servers, was used in the analysis. In the EEG, spikes were automatically detected using Persyst Spike Detector P13 (Persyst, San Diego, CA, U.S.A.). The spikes were detected in all available EEGs of the patients, so also during spike bursts and ictal events, both clinical and subclinical. Single spikes with a spike probability indicating how likely the detected event is a genuine epileptiform event according to the Persyst Spike Detector P13 lower than 0.5 and those who had 1 or more bad channels were rejected. A channel was defined as bad when the standard deviation exceeded

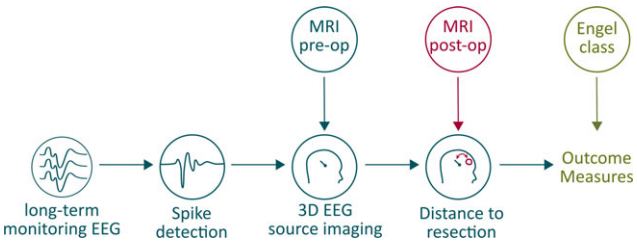

Figure 1.
The proposed framework for automated EEG analysis of long-term EEG recordings. From the long-term EEG, the spikes are automatically detected using the Persyst P13 spike detector and averaged afterward. The T1-weighted MRI is used to build a patient-specific head model to perform ESI to localize the underlying source of the averaged spikes. The spike localization is compared to the resection delineated from the postoperative MRI. Given the surgical outcome of the patients, evaluation measures are computed.

five times the median standard deviation of all channels during the considered spike. The remaining single spikes were averaged per type.

Next we joined spike clusters when the scalp topography was highly similar, meaning if the correlation of the scalp maps at the peak of the spikes exceeded 0.9. Two clusters, the first one consisting of the most frequently occurring and the other of the second-most frequently occurring type of spikes, were selected for each patient. The events belonging to the same cluster were averaged in each patient and used for subsequent analysis. For each cluster we calculated the similarity measure that showed how the morphology of the individual spikes corresponds with that of the averaged spike. The similarity measure was calculated as the mean of correlation between the individual and the averaged spike in the 200-ms interval around the peak of the averaged spike.

We performed two additional analyses to quantify the performance of the spike detection: (1) the detected spikes were scored by an expert electrophysiologist (KV) to confirm or deny whether the spike was a genuine interictal epileptiform discharge, and (2) the type of spike was compared to the type of interictal EEG findings mentioned in the clinical report of the patient's stay at the epilepsy monitoring unit written by the epileptologist. The results of the additional analyses did not influence further analysis, meaning that the results were not considered in the automated analysis pipeline.

EEG source imaging

The sources of the detected spike clusters were estimated using EEG Source Imaging (see Data S1 for details). The distance from the ESI locations, that is, the source point with maximum activity, to the border of the resection, manually delineated based on a postoperative MRI, was computed: d_{clus1_peak}, d_{clus1_half}, d_{clus2_peak}, and d_{clus2_half}. We also calculated the resected volume in each patient. For each spike cluster we also computed the spreading measure that indicates how consistent the ESI of single spikes is. The spreading measure was calculated as the mean distance from the ESI location of the single spikes to the ESI location of the averaged spike. Here we only considered the 100 single spikes that had highest morphology correlation with the averaged spike.

We performed a two-way repeated-measures ANOVA in SPSS Statistics 23 to test the influence of spike occurrences (most frequent spike cluster 1 vs. less frequent spike cluster 2) and timing at which to perform ESI (peak vs. half-rising time of the spike) on the distance to the resection in patients with favorable outcome (Engel Class 1).

Outcome measures

On the basis of the calculated distances from the ESI location to the resection, the sensitivity, specificity, positive prediction value (PPV), negative prediction value (NPV), and diagnostic odds ratio (OR) of the described method to localize the EZ was assessed. A patient with Engel class I outcome with localization inside or outside the vicinity of the resection (within 10 mm) was considered a true positive (TP) or false negative (FN), respectively. Engels class II, III, and IV patients are considered false positives (FP) or true negatives (TN) if the localization was found inside or outside the vicinity of the resection, respectively. From the TN, TP, FN, and FP, we calculated the sensitivity, specificity, PPV, NPV, and the diagnostic OR, which expresses the predictive power of a test.

The distance to the border of the resection was calculated and not the one to the center of the resection, because when a brain region is removed, it is not certain which part of it corresponded to the EZ. If the patient is seizure free after surgery, one can assume that the EZ was included in the resection, but it remains uncertain whether the middle part was more epileptogenic compared to the removed border parts. For this reason we choose to calculate the distance to the border instead of to the centroid of the resection volume.

The above introduced evaluation measures were calculated for each of the 4 following groups: spike cluster 1 at peak and half-rising time, spike cluster 2 at peak and half-rising time. We did not take the scoring of the spikes by the neurologist into account, meaning all spikes were included to calculate the outcome measures. Furthermore, we also calculated the outcome measures when simultaneously considering the results of the two spike clusters. This led to the two following groups: spike cluster 1+ spike cluster 2 at the peak and half-rising time of the spike. Here, an Engel class I patient is considered a TP when one of the localizations was inside the resection. If both locations are outside the resection, the patient is considered a FN. For Engel classes II, III, and IV, a patient is a TN if both localizations are outside the resection and a FP when one or two of the localizations are inside the resection.

We performed logistic regression modeling in SPSS Statistics 23 to identify factors that were predictive for favorable outcome. The investigated independent factors were distance of the ESI solution to the closest resection margin of spike cluster 1 at the peak, number of detected events in cluster 1, the resection volume, the similarity measure, the spreading measure, and at which hospital the patient underwent the presurgical evaluation. Finally, we performed linear regression analysis to investigate factors that are predictive for the distance to the resection. The investigated independent factors here were the number of detected events in spike cluster 1, the scoring of the neurologist, the similarity measure, the spreading measure, at which hospital the patient was operated, and the resection volume.

Results

Detected spikes

The duration of available EEGs used for analysis differed between hospitals: in Ghent the median duration of EEG

recordings was 57 h, whereas in Geneva it was 6 h. The duration of the analyzed EEG epochs in all 32 patients is shown in Table 1.

The type and the number of detected spikes are shown in Table 2 for all patients. The median number of detected spikes in the patients was 740 (42/h) and 192 (6/h) for spike clusters 1 and 2, respectively. For the patients recorded in Ghent, the median number of detected spikes was 1,783 (26/h) and 207 (4/h), while for those recorded in Geneva it was 539 (100/h) and 177 (42/h), for spike clusters 1 and 2, respectively.

In Fig. S2 the detected spike clusters in 10 patients are shown as an example. Patients 2, 5, and 6 have right frontotemporal spikes; Patients 15, 18, and 27 have left frontotemporal spikes. The expert electrophysiologists indicated that 84% of detected spikes of cluster 1 resembled genuine epileptiform interictal activity. For example, spike cluster 1 was scored as not being genuine epileptiform activity in Patients 11 and 17, whereas in all others patients in Fig. S2 it was regarded as a genuine epileptic spike.

In 28 of the 32 patients, the detected spikes were concordant with the interictal findings mentioned in the report of the long-term EEG monitoring. For instance, in the report of Patient 31 it was indicated that there were more left temporal spikes than right temporal spikes. In this case 539 spikes type F7-T7 and 155 spikes type F4 were detected. In 2 patients, namely, Patient 6 and Patient 18, no interictal epileptiform discharges were noticed in the long-term EEG, according to the report. In both cases, spikes were detected in the EEG by Persyst P13. In Patient 6, 618 (15.8/h) spikes of type F8-T4 and 32 (0.8/h) spikes of type F7 were detected; in Patient 18, 251 (6/h) spikes of type T3-F7 and 16 (0.4/h) spikes of type T4 were detected. In Patient 6 the detected events were not genuine spikes, but cardiac artefacts. In Patient 18, the electrophysiologist confirmed that spike cluster 1 was composed of genuine epileptiform discharges. However, these discharges were detected during ictal epochs, explaining why they were not mentioned in the long-term monitoring report as interictal epileptiform discharges. Spike cluster 2 in Patient 18 was not a genuine epileptiform discharge. In 2 other patients, namely, Patient 12 and Patient 24, the detected spikes were partly inconsistent with the interictal findings. The visual analysis report indicated in Patient 12 that high-voltage spike-wave discharges left frontotemporal over F7 and Fp1were observed, and the software detected more spikes of the type right-frontotemporal (F8-T4) compared to left frontotemporal (F7-T3). In Patient 24, the report mentioned central parietal midline spikes, while the software detected left frontotemporal (F7) and left temporal (T7) spikes.

Distance to the resection

In Fig. 2 the histograms of the distances to the resection are shown for the patients with good and bad outcomes. Despite the fact that only 8 patients with Engel Class II, III, or IV are included in the study, we can see that the distances to the resection are larger than in the patients with Engel Class I outcomes. Within the favorable outcome patients, the statistical test identified spike occurrence and spike timing as a significant factor ($p < 0.05$), meaning that the distance to the resection for spike cluster 1 is significantly smaller compared to that of spike cluster 2 and that the distance to the resection is significantly smaller at the peak of the spike compared to at the half-rising time of the spike ($p < 0.05$). We did not find a significant interaction effect between spike occurrence and spike timing for ESI.

The distances to the resection in individual patients are depicted in Table 2. The median distance to resection for patients of Engel Class I for spike cluster 1 was 7 mm and 15 mm at the time of the peak and the half-rising time of the spike, respectively. For cluster 2 these values increased to 27 and 26, respectively. For patients of Engel Classes II, III and IV, the median distances were 36 mm and 36 mm for cluster 1 and 32 mm and 26 mm for cluster 2, at peak and half-rising time, respectively.

Outcome measures

The outcome measures are depicted in Table 3. The sensitivity to localize the EZ from ESI of spike cluster 1 is 70% at the peak of the spike and drops to 38% when we localize at the half-rising time. The specificity is 100% at the time of the peak and at the half-rising time. Spike cluster 2 results in a poor sensitivity. However, considering spike cluster 2 together with spike cluster 1 increased the number of TPs. The second spike cluster was able to localize the EZ in 3 of the 28 patients, namely, in Patients 9, 12, and 21, where spike cluster 1 was not able to localize the EZ. At the peak of the spike, we achieve a sensitivity of 79% when considering the clusters together, while at the half-rising time the sensitivity was only 46%. At the time of the peak and at half-rising time, the specificity dropped to 75% and 88%, respectively. We achieve the best results when both spikes are localized at the peak of the spike, namely, sensitivity 79%, specificity 75%, PPV 90%, NPV 55%, and diagnostic OR 11.4.

Statistical testing indicated that ESI of spike cluster 1 at the time of the peak was a predictor of favorable outcome ($p = 0.003$). The adjusted prognostic OR was 13.63. The factors resection volume, number of detected spikes in spike cluster 1, and hospital at which the presurgical evaluation was performed did not have a significant predictive value. Linear regression analysis showed that the spreading measure was a predictor of the distance to the resection ($p = 0.022$). The lower the spreading measure, the lower the distance to the resection margin.

Patient examples

In this section we present the cases of 2 individual patients: Patient 13 and Patient 15.

Table 2. The patient individual results of the automated EEG analysis

	Cluster 1									Cluster 2								
Pat ID	Type	Max ampl	#detec	#detec / hour	Scoring	Peak (mm)	Half (mm)	Sim (%)	Spread (mm)	Type	Max ampl	#detec	#detect/h	Scoring	Peak (mm)	Half (mm)	Sim (%)	Spread (mm)
1	F8	F8	116	1.9	Yes	41	28	50	34	F7	F7	54	0.9	Yes	41	43	48	22
2	F8-T4	F8	77	1.4	Yes	0	0	62	18	–	–	–	–	–	–	–	–	–
3	F8-T4	TP10	25.137	399.0	Yes	0	2	69	12	F7	F7	16	0.3	No	51	26	43	47
4	T4	T4	504	6.1	No	0	0	36	16	F8	F8	392	4.7	Yes	0	24	40	13
5	F8-Fp2	F8	1.968	34.5	Yes	0	1	60	15	T4-T6	T4	340	6.0	Yes	2	4	56	15
6	F8-T4	O1	618	15.8	No	55	62	64	9	F7	O1	32	0.8	No	38	44	56	15
7	T4-F8	TP10	2.141	25.7	Yes	43	84	34	32	T5-O1	FT9	207	2.5	No	66	82	33	38
8	F8-T4	F8	10.974	142.1	Yes	8	8	61	18	Fp2	FT10	60	0.8	Yes	18	8	63	44
9	F8-T4	F8	5.027	60.4	Yes	16	28	55	15	Fp2-F4	Fp2	1.689	20.3	Yes	9	16	59	13
10	T3	T3	637	7.7	Yes	57	91	41	25	F7	F7	395	4.7	Yes	69	78	37	20
11	T3	T3	1.783	82.0	No	9	33	51	14	T5	T5	565	26.0	No	26	25	54	15
12	F8-T4	FT10	1.874	25.7	No	38	45	32	22	F7-T3	F7	559	7.7	No	5	19	37	18
13	F8	F8	4.638	55.7	Yes	9	13	38	16	T4	T4	562	6.8	Yes	13	55	34	26
14	F8-T4	F8	337	12.7	Yes	0	0	45	14	T3	T3	42	1.6	No	63	72	31	45
15	F7-T3	F7	2.781	114.3	Yes	9	15	49	22	F8-T4	FT10	208	8.5	No	71	60	43	41
16	T3	T3	2	3.6	Yes	0	24	84	10	–	–	–	–	–	–	–	–	–
17	T6-O2	T6	104	6.3	No	33	56	56	19	F7	F7	33	2.0	No	41	38	57	21
18	T3-F7	TP9	251	6.0	Yes	2	50	47	20	T4	T4	16	0.4	No	40	11	49	37
19	F7	F7	7	0.8	No	66	51	46	33	Fp2	Fp2	6	0.7	No	44	26	48	26
20	T4-F8	T4	7.062	293.0	Yes	6	16	44	14	F4-Fp2	F4	94	3.9	No	34	49	39	42
21	C3-F3	C3	49.553	545.5	Yes	13	15	52	9	F7	F7	40.786	449.0	Yes	3	10	56	9
22	T3	T3	4.713	75.8	Yes	28	45	32	17	O1-T5	O1	4.446	71.5	Yes	26	26	30	18
23	F7-T3	F7	73	49.2	Yes	10	6	50	26	F4	T9	4	2.7	Yes	0	26	55	36
24	F7	F7	89	10.0	Yes	52	48	38	20	T7	F7	57	6.4	Yes	49	49	39	34
25	T8	T8	67	35.0	Yes	0	58	30	36	F8	F8	31	16.2	Yes	0	0	45	32
26	F7	F7	359	73.5	Yes	33	30	39	33	T7	T7	300	61.4	Yes	19	53	38	27
27	T7-F7	T7	1.215	215.0	Yes	0	2	34	19	F4-Fz	F4	128	22.7	No	28	22	35	39
28	P4	P4	843	100.2	Yes	27	25	24	47	Pz	Pz	412	49.0	Yes	16	17	32	33
29	P7-O1	P7	1.912	501.0	Yes	0	0	50	16	T7	T7	1.602	419.7	Yes	5	6	50	24
30	T8-F8	T8	370	29.3	Yes	2	13	38	25	F7	F7	177	14.0	No	35	45	45	22
31	F7-T7	F7	539	146.3	Yes	13	16	54	15	F4-F3	Fz	155	42.1	No	44	39	42	40
32	P7	P7	2.751	366.8	Yes	44	23	43	51	F7	F7	332	44.3	Yes	0	0	42	20

The first column shows the patient identification number. There are 2 large columns that show the results of spike cluster 1 and spike cluster 2. Each column has several subcolumns that show the following information: type = the type of detected spikes; max ampl = the maximum amplitude of the average spikes; #detec = the number of detected single spikes of this type; #detec/hour = number of detections per hour; scoring = the scoring of the neurologist (yes means genuine spike, no means not a spike); peak (mm) = distance to the resection at the peak of the spike; half (mm) = distance to the resection at the half-rising phase of the spike; sim (%) = similarity measure of the spike; spread (mm) = spread measure of the spike.

Epilepsia Open, 2(3):322–333, 2017
doi: 10.1002/epi4.12066

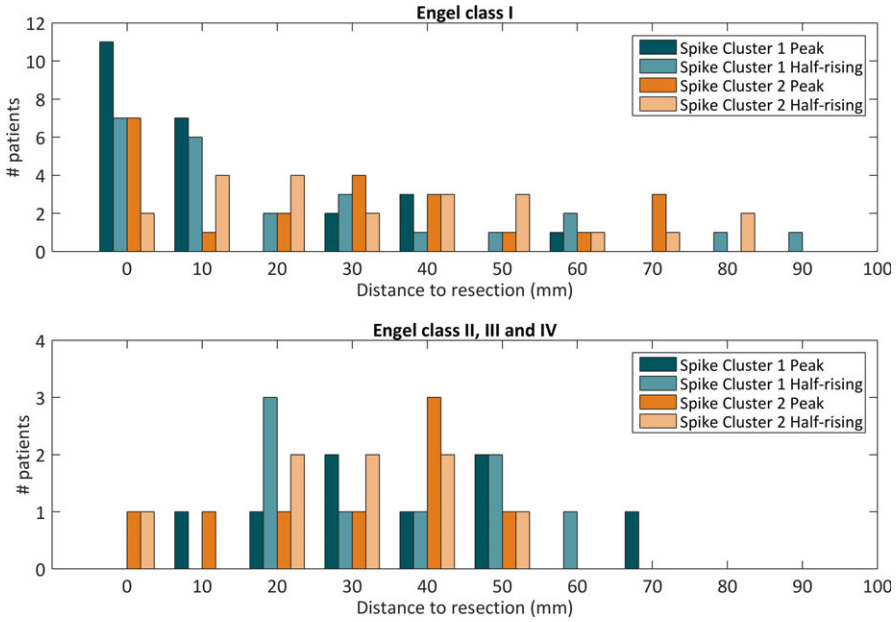

Figure 2.
Histogram of the distances to the resection for spike clusters 1 and 2 during the peak and the half-rising of the spike for good-outcome patients (Engel class I) and bad-outcome patients (Engel classes II, III, and IV).

Table 3. The outcome measures to localize the EZ using the described methodology

	Clus 1 peak	Clus 1 half-rising	Clus 2 peak	Clus 2 half-rising	Clus 1 + 2 peak	Clus 1 + 2 half-rising
TP	16	9	7	4	19	11
FN	7	15	15	17	5	13
TN	8	8	6	7	6	7
FP	0	0	2	1	2	1
Sens	70%	38%	32%	19%	79%	46%
Spec	100%	100%	75%	88%	75%	88%
PPV	100%	100%	78%	80%	90%	92%
NPV	53%	35%	29%	29%	55%	35%
OR	/	/	1.4	1.6	11.4	5.9

FN, false negative; FP, false positive; NPV, negative predictive value; OR, odds ratio; PPV, positive predictive value; Sens, sensitivity; Spec, specificity; TN, true negative; TP, true positive.

Patient 13

In this patient, 4,638 single spikes with phase reversal over F8 and 562 with phase reversal over T4 were detected. The spike and corresponding localization are shown in the top panel of Fig. 3. The two clusters of detected spikes have similar morphology, although differences can be noticed especially in traces F8-T4, Fp2-F4, and T6-O2. The patient had a selective right amygdalohippocampectomy and has been seizure free since. The resection volume was only 5 cm^3. The localization of the spikes corresponded with the resection. The distance to the resection for spike cluster 1 was 9 mm and 13 mm when the spike was localized at the peak and the half-rising phase, respectively. Spike cluster 2 was localized close to the resection when ESI was performed at the time of the peak (d = 13 mm), and at the half-rising phase the distance to the resection was large (d = 55 mm).

Patient 15

In the EEG of Patient 15, 2,781 left frontotemporal spikes (F7-T3) and 208 contralateral spikes (F8-T4) were detected. The patient had a small left temporal lesionectomy with a resection volume of 2.6 cm^3 and has been seizure-free since. The spike clusters and corresponding localization are shown in the bottom panel of Fig. 3. At the peak, spike cluster 1 was localized close to the resection (d = 7 mm) and a bit farther away at the half-rising time (d = 15 mm). Spike cluster 2 was localized far from the resection when localized at the peak (d = 71 mm) and at the half-rising time (d = 60 mm).

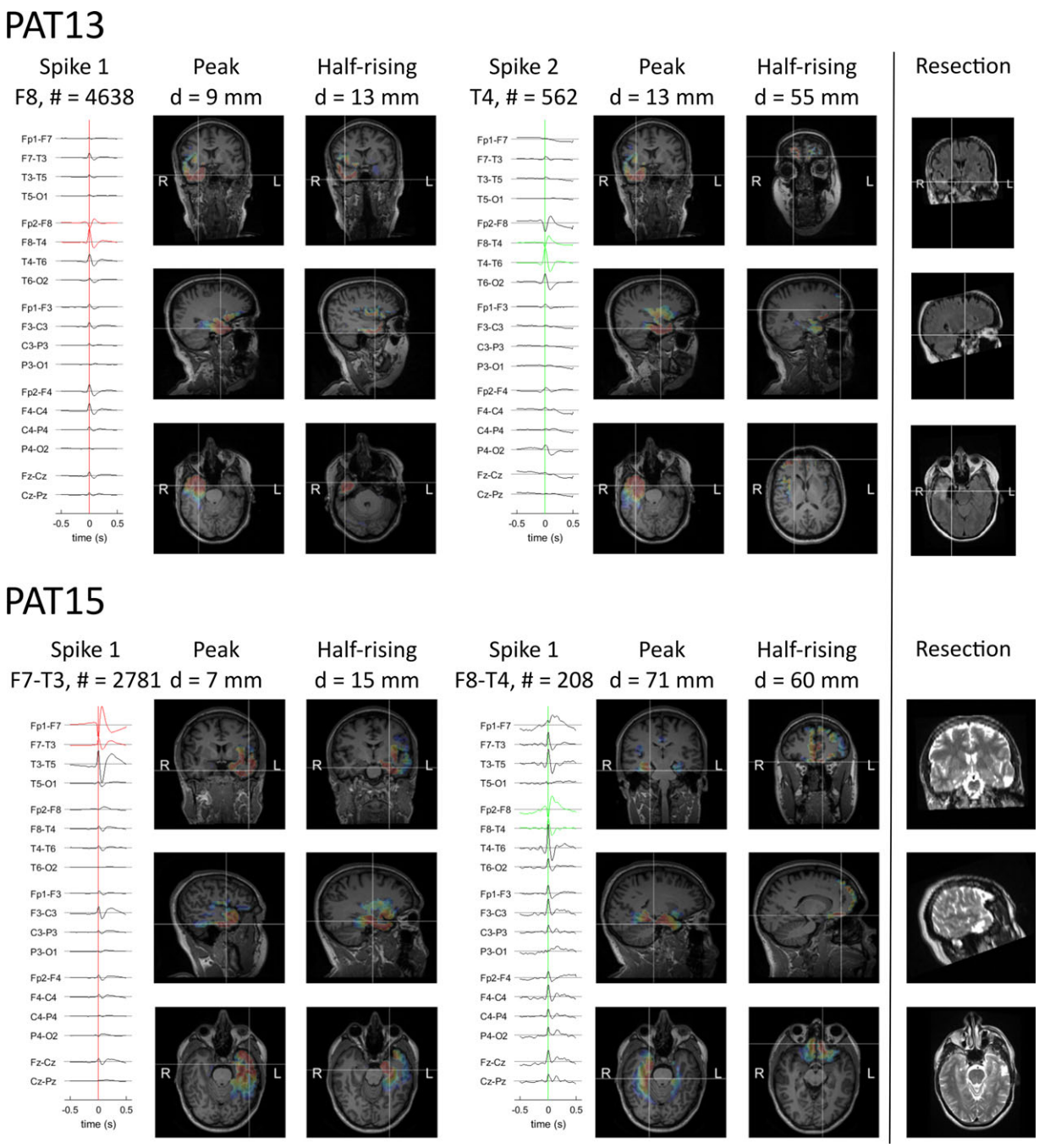

Figure 3.
Example of the automatic spike detection and subsequent ESI to localize the EZ. Patient 13 had right temporal lobe epilepsy; Patient 15 had a left temporal lesionectomy. The localizations at the time of the peak and at the half-rising time of the spike are shown. The distance to the resections (*d*) is indicated above the figure.
Epilepsia Open © ILAE

Discussion

Outcome measures

The presented method automatically detects spikes in long-term EEG recordings and subsequently performs ESI that allows localizing the sources of the spikes. The results of the automated EEG analysis can be used to help identify the EZ with a sensitivity of 70% and a specificity of 100% when only the most frequent spike cluster was taken into account. The sensitivity increased to 79% when both spike cluster 1 and spike cluster 2 were considered, while the specificity dropped to 75%. These outcome measures are

higher than earlier findings by Brodbeck et al.,[5] who reported a sensitivity of 66% and specificity of 54% when spikes marked in long-term EEG were used to localize the EZ. This can result from several reasons: the use of more realistic EEG forward model (6 tissues segmented from individual MRI), the higher signal-to-noise ratio of the averaged spikes (more spikes are detected by the algorithm than are usually marked by the neurologist), the natural variability in different investigated populations, or the use of a different inverse method.

It has been shown that the sensitivity and specificity increase to 84% and 88%[5] or to 88% and 47%[6] when high-density EEG recordings are analyzed. However, not all epilepsy centers have the required high-density EEG equipment, and long-term recordings up to several days with high-density EEG nets are more difficult than with clinical telemetry using glued electrodes. Nevertheless, there is a trend in using an increased number of electrodes, also for video-EEG monitoring. The use of low temporal electrodes is likely to be critical for ESI accuracy on telemetry recordings. Although our proposed method can be applied to high-density EEG recordings, future studies are required to quantify the performance of our method in such a setting.

The performance of our method to localize the EZ is in the same range as other noninvasive techniques that are part of the presurgical evaluation protocol.[6] The sensitivity to localize the EZ for interictal PET ranges between 60% and 100% and for ictal SPECT from 66% to 97%.[16,17] In the study of Brodbeck et al.[5] in 152 patients, the sensitivity and specificity of ictal SPECT was 58% and 47%; of interictal PET, 68% and 44%; and of structural MRI, 76% and 53%, respectively. The proposed automated analysis of the EEG is therefore equally informative as other noninvasive imaging methods. Although the sensitivity and specificity of each individual technique are high, we need to keep in mind that during the presurgical evaluation the results of all presurgical evaluation techniques are combined and not used separately. Nevertheless, because in most epilepsy centers, clinical EEG and structural MRI are recorded in the standard protocol in patients, these data are available. Running the proposed automated EEG analysis is an easy way to get more out of the recorded data.

State-of-the-art individual head models with six different tissue classes (scalp, skull, cerebrospinal fluid [CSF], gray matter, white matter, and air) were constructed to perform the ESI. We did model the air cavities/sinuses in the patients because not modeling them could introduce focal localization errors in the frontal and temporal regions.[18] The skull was modeled as a single isotropic layer and not anisotropic or as 3 layers, because we recently showed that more complex skull modeling approaches did not lead to significant differences in the localization of the irritative zone from clinical EEG data recorded with low spatial sampling.[19] We used a skull conductivity of 0.0105 S/m according to Dannhauer et al.,[20] who calculated the optimal isotropic conductivity on the basis of the conductivity measurements of the spongy and hard bone of Ahktari et al.[21] It must be noted that these conductivity values were measured in dead bone tissue. Hoekema et al.[22] performed measurements in living skull fragments during bone flap surgery and showed that the conductivity values ranged from 0.032 S/m to 0.080 S/m and that they vary with age. These values are a factor 3 to 8 times higher than the conductivity values used in our study. Using these higher skull conductivity values would result in the sources being estimated more laterally, less deep in the brain.

A limitation of the study is that the sensitivity and specificity were calculated using the vicinity of the resected zone, inside 10 mm of the resection border. This was chosen because the spatial resolution of ESI is in the centimeter range, and it has been shown that <64 electrodes cannot be used for sublobar localization.[23] Brain shift after resective surgery might also introduce a localization error on the postoperative MRI that is represented in the 10-mm margin. Furthermore, most of the resections were small and located deep inside the brain. In some cases, especially for the patients who had an amygdalohippocampectomy, it is still debated whether activity from these deep regions can be picked up by scalp EEG.[24–26] Despite this limitation, localizing the spikes in the vicinity (1-cm range) of the EZ is useful for clinical diagnosis and helps identify the EZ. In Patients 8, 11, 13, 18, 20, 23, and 30 who had a selective amygdalohippocampectomy, the localization of spike cluster 1 was within 1 cm of the resection, which is useful for clinical decision making, and therefore we considered these cases as true positives. In 1 other patient, namely, Patient 15, the localization was 7 mm away from a small lesion seen in the MRI. We considered this patient also a true positive, because ESI was pinpointing the lesion. In all cases where the distance to the resection was higher than 0 mm and lower than 10 mm, the spike cluster was localized inside the same brain lobe where the resection took place. In all true positive cases that had a big resection (larger than 10 cm^3), the source of cluster 1 spikes was estimated to have fallen within the brain tissue that was ultimately resected. This means that the <1 cm from the border of the resection criterion was only used in cases that had a small resection and was not needed in the big resection cases.

In our study we assumed in patients with Engel class I outcomes that the epileptogenic region was included in the resection, by definition. However, we can only guess as to the precise volume of the epileptogenic zone. Could a smaller resection have led to seizure freedom? Did the resection induce a change in structural or functional brain connectivity that rendered the patient seizure free? These questions cannot be answered and, therefore, we should be cautious interpreting the epileptogenic focus localization results based on resection volumes. Nevertheless, the localization of sources of epileptic spikes using ESI on high-density EEG allows formally delineating the irritative zone and is a

good, but not absolute, surrogate of the seizure onset zone.[27] ESI of interictal spikes can play an important role, and its localization in the resection zone is strongly associated with seizure-free outcome in several studies.[5,6] Our automated method suggests that this might also be the case with low-density EEG recordings. Most resections in our study were very small and up-to-date, considering that the volume of brain tissue resected as one of the possible determinants of outcome measures in resective epilepsy surgery is consistent with best clinical practice as we see it.

We showed that the automated framework for spike detection and subsequent localization is useful to localize the epileptogenic region. However, the proposed methodology cannot be used to determine the extent of the epileptogenic focus. A promising EEG and MEG source localization technique based on maximum entropy on the mean could help in determining the extent of the EZ, as was shown in simulations[28,29] and in 5 patients using MEG localization of spikes.[30] The MEG localization extent corresponded to intracranial EEG recordings in 4 out of the 5 investigated patients.

The proposed method is completely automated and does not require manual intervention except for manually adjusting the electrode positions on the head model. This manual adjustment can be avoided by recording the actual positions of the electrodes during the video-EEG monitoring. Unfortunately, the measurements were not available in both epilepsy centers. Advantages of the automated analysis are objectivity and reliability. Analyzing the same EEG twice will lead to the same results. A possible disadvantage of the automatic spike detection technique is that spikes can be missed by the software. We suggest using the software in combination with visual analysis of the EEG. If visual analysis confirms the output of the automated method, the results can be considered valuable; if not, the results should be carefully interpreted.

Automated spike detection

There is a notable difference in the length of the analyzed EEG recordings and the number of detected spikes per hour between Ghent University Hospital and the University Hospital of Geneva. This results from the fact that in Ghent more EEG data per patient are archived on the hospital servers compared to in Geneva. In Geneva the segments are carefully selected to contain a lot of epileptiform activity before they are stored. This led to the difference of number of detected spikes per hour between the hospitals.

The advantage of automatic detection of the interictal discharges from long-term EEG recordings is that the detected number of a certain spike type can be high. For example, in our study up to 49,553 single spikes were detected in Patient 21. The high number of detections increases the signal-to-noise ratio of the spike, which is advantageous to performing subsequent ESI. Furthermore, automated detection of spikes allows ranking the spike clusters based on occurrences of single events. This is important given the fact that the spike cluster with most occurrences has a higher probability to be linked to the EZ.[31,32] We confirmed this finding by showing that the distance to the resection was significantly smaller for the cluster with the highest spike count compared to that with the second highest one.

Conclusion

We showed that automated long-term EEG analysis has a high sensitivity and specificity to localize the epileptogenic zone and therefore deserves a more prominent role during the presurgical evaluation of focal epilepsy.

Acknowledgments

This project received funding from the European Union's Horizon 2020 research and innovation program under the Marie Sklodowska-Curie grant agreement No. 660230. The study was supported by the Swiss National Science Foundation (MS: 163398, 140332, 146633; SV: CRSII5_170873, 169198). The study received funding from Fonds Wetenschappelijk Onderzoek–Vlaanderen (grant V405016N).

Disclosure of Conflicts of Interest

The authors P.v.M., G.S., V.K., P.B., S.V., M.S. are shareholders of Epilog NV. The remaining authors have no conflicts of interest. We confirm that we have read the Journal's position on issues involved in ethical publication and affirm that this report is consistent with those guidelines.

References

1. Rosenow F. Presurgical evaluation of epilepsy. *Brain* 2001;124:1683–1700.
2. Rosenow F, Bast T, Czech T, et al. Revised version of quality guidelines for presurgical epilepsy evaluation and surgical epilepsy therapy issued by the Austrian, German, and Swiss Working Group on Presurgical Epilepsy Diagnosis and Operative Epilepsy Treatment. *Epilepsia* 2016;57:1215–1220.
3. Michel CM, Murray MM. Towards the utilization of EEG as a brain imaging tool. *NeuroImage* 2012;61:371–385.
4. Plummer C, Harvey AS, Cook M. EEG source localization in focal epilepsy: where are we now? *Epilepsia* 2008;49:201–218.
5. Brodbeck V, Spinelli L, Lascano AM, et al. Electroencephalographic source imaging: a prospective study of 152 operated epileptic patients. *Brain* 2011;134:2887–2897.
6. Lascano AM, Perneger T, Vulliemoz S, et al. Yield of MRI, high-density electric source imaging (HD-ESI), SPECT and PET in epilepsy surgery candidates. *Clin Neurophysiol* 2016;127:150–155.
7. Kirchberger K, Hummel C, Stefan H. Postoperative multichannel magnetoencephalography in patients with recurrent seizures after epilepsy surgery. *Acta Neurol Scand* 1998;98:1–7.
8. Knowlton RC, Elgavish RA, Bartolucci A, et al. Functional imaging: II. Prediction of epilepsy surgery outcome. *Ann Neurol* 2008;64:35–41.
9. Mouthaan BE, Rados M, Barsi P, et al. Current use of imaging and electromagnetic source localization procedures in epilepsy surgery centers across Europe. *Epilepsia* 2016;57:770–776.
10. Pascual-Marqui RD, Michel CM, Lehmann D. Low resolution electromagnetic tomography: a new method for localizing electrical activity in the brain. *Int J Psychophysiol* 1994;18:49–65.
11. Pascual-Marqui RD, Lehmann D, Koukkou M, et al. Assessing interactions in the brain with exact low-resolution electromagnetic tomography. *Philos Trans A Math Phys Eng Sci* 2011;369:3768–3784.

12. Pascual-Marqui RD. Standardized low-resolution brain electromagnetic tomography (sLORETA): technical details. *Methods Find Exp Clin Pharmacol* 2002;24:5–12.
13. de Peralta G, Menendez R, Murray MM, et al. Electrical neuroimaging based on biophysical constraints. *NeuroImage* 2004;21:527–539.
14. Mosher JC, Leahy RM. Recursive MUSIC: a framework for EEG and MEG source localization. *IEEE Trans Biomed Eng* 1998;45:1342–1354.
15. Birot G, Spinelli L, Vulliémoz S, et al. Head model and electrical source imaging: a study of 38 epileptic patients. *Neuroimage Clin* 2014;5:77–83.
16. Knowlton RC. The role of FDG-PET, ictal SPECT, and MEG in the epilepsy surgery evaluation. *Epilepsy Behav* 2006;8:91–101.
17. la Fougère C, Rominger A, Förster S, et al. PET and SPECT in epilepsy: a critical review. *Epilepsy Behav* 2009;15:50–55.
18. Montes-Restrepo V, van Mierlo P, Strobbe G, et al. Influence of skull modeling approaches on EEG source localization. *Brain Topogr* 2013;27:95–111.
19. Montes-Restrepo V, Carrette E, Strobbe G, et al. The role of skull modeling in EEG source imaging for patients with refractory temporal lobe epilepsy. *Brain Topogr* 2016;29:572–589.
20. Dannhauer M, Lanfer B, Wolters CH, et al. Modeling of the human skull in EEG source analysis. *Hum Brain Mapp* 2010;32:1383–1399.
21. Akhtari M, Bryant HC, Mamelak AN, et al. Conductivities of three-layer live human skull. *Brain Topogr* 2002;14:151–167.
22. Hoekema R, Wieneke GH, Leijten FS, et al. Measurement of the conductivity of the skull, temporarily removed during epilepsy surgery. *Brain Topogr* 2001;16:29–38.
23. Lantz G, Grave de Peralta R, Spinelli L, et al. Epileptic source localization with high density EEG: how many electrodes are needed? *Clin Neurophysiol* 2003;114:63–69.
24. Pacia SV, Ebersole JS. Intracranial EEG substrates of scalp ictal patterns from temporal lobe foci. *Epilepsia* 1997;38:642–654.
25. Jan MM, Sadler M, Rahey SR. Electroencephalographic features of temporal lobe epilepsy. *Can J Neurol Sci* 2010;37:439–448.
26. Yamazaki M, Tucker DM, Fujimoto A, et al. Comparison of dense array EEG with simultaneous intracranial EEG for interictal spike detection and localization. *Epilepsy Res* 2012;98:166–173.
27. Megevand P, Spinelli L, Genetti M, et al. Electric source imaging of interictal activity accurately localises the seizure onset zone. *J Neurol Neurosurg Psychiatry* 2013;85:38–43.
28. Chowdhury RA, Lina JM, Kobayashi E, et al. MEG source localization of spatially extended generators of epileptic activity: comparing entropic and hierarchical Bayesian approaches. *PLoS ONE* 2013;8:e55969.
29. Chowdhury RA, Merlet I, Birot G, et al. Complex patterns of spatially extended generators of epileptic activity: comparison of source localization methods cMEM and 4-ExSo-MUSIC on high resolution EEG and MEG data. *NeuroImage* 2016;143:175–195.
30. Grova C, Aiguabella M, Zelmann R, et al. Intracranial EEG potentials estimated from MEG sources: a new approach to correlate MEG and iEEG data in epilepsy. *Hum Brain Mapp* 2016;37:1661–1683.
31. Asano E, Muzik O, Shah A, et al. Quantitative interictal subdural EEG analyses in children with neocortical epilepsy. *Epilepsia* 2003;44:425–434.
32. Marsh ED, Peltzer B, Brown Iii MW, et al. Interictal EEG spikes identify the region of electrographic seizure onset in some, but not all, pediatric epilepsy patients. *Epilepsia* 2010;51:592–601.

Supporting Information

Additional Supporting Information may be found in the online version of this article:

Data S1. EEG source imaging.

Figure S1. The electrode configuration used during the long-term EEG monitoring.

Figure S2. Example of automatically detected spikes in 10 patients.

Figure S3. Example of automatically generated head model with 6 tissues from the T1-weighted MRI image of Patient 3 (RTLE, seizure-free postoperatively).